

## **Supplementary material to:**

# **Injection strategy - a driver of atmospheric circulation and ozone response to stratospheric aerosol geoengineering**

Ewa M. Bednarz<sup>1,2,3</sup>, Amy H. Butler<sup>2</sup>, Daniele Visioni<sup>3,4</sup>, Yan Zhang<sup>3</sup>, Ben Kravitz<sup>5,6</sup>, Douglas G. MacMartin<sup>3</sup>

1. Cooperative Institute for Research in Environmental Sciences (CIRES), University of Colorado Boulder, Boulder, CO, USA

2. National Oceanic and Atmospheric Administration (NOAA), Chemical Sciences Laboratory (CSL), Boulder, CO, USA

3. Sibley School of Mechanical and Aerospace Engineering, Cornell University, Ithaca, NY, USA

4. National Center for Atmospheric Research (NCAR), Atmospheric Chemistry Observations and Modelling (ACOM), Boulder, CO, USA

5. Department of Earth and Atmospheric Sciences, Indiana University, Bloomington, IN, USA

6. Atmospheric Sciences and Global Change Division, Pacific Northwest National Laboratory, Richland, WA, USA

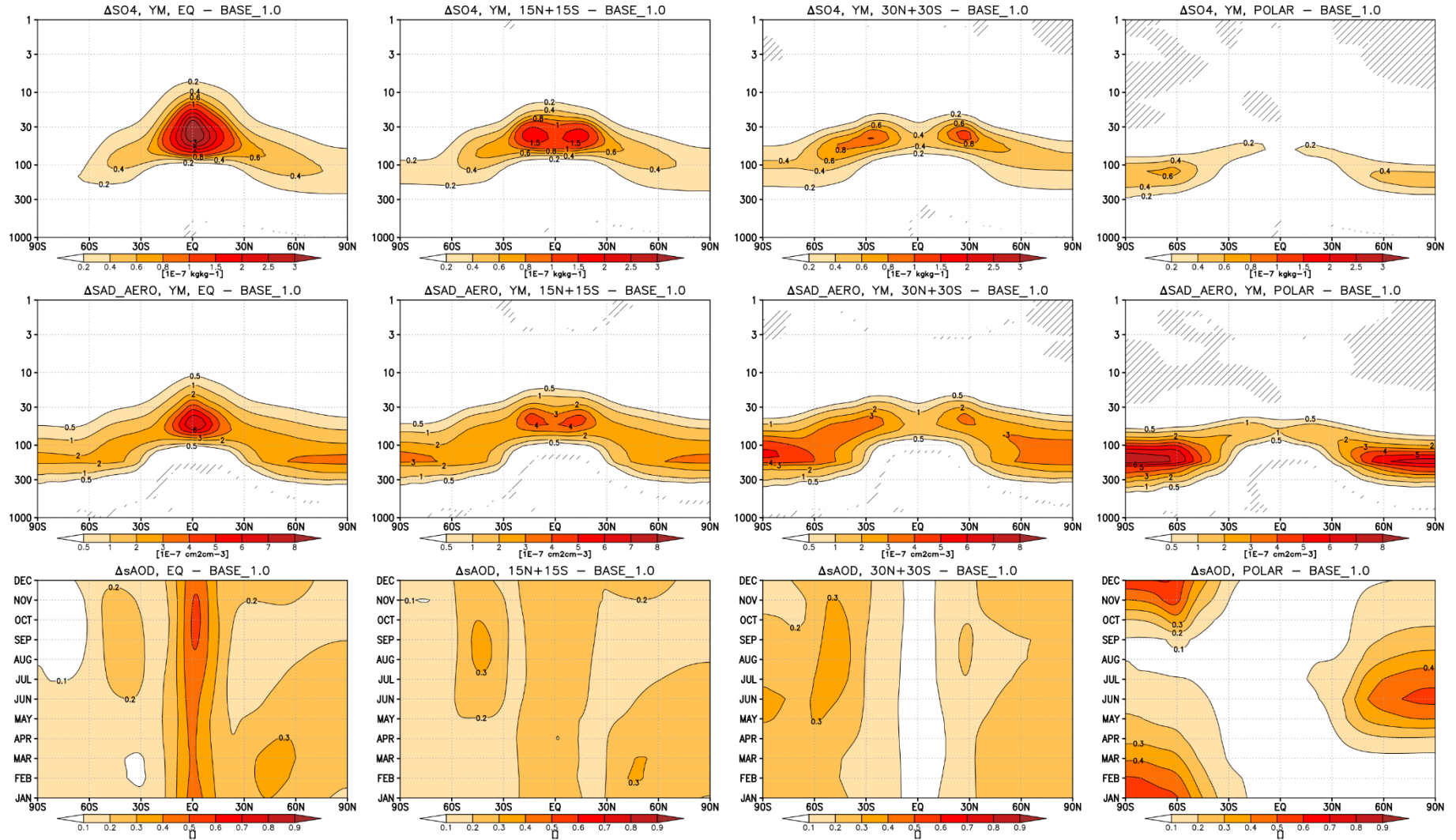


**Figure S1.** (Top) Yearly mean changes in sulfate mass mixing ratios, (middle) yearly mean changes in sulfate surface area density, and (bottom) spatiotemporal evolution of simulated AOD changes in EQ, 15N+15S, 30N+30S and POLAR strategy compared to the baseline period

(2008-2027). Hatching indicate regions where the response is not statistically significant, taken as smaller than  $\pm 2$  standard errors of the difference in means.

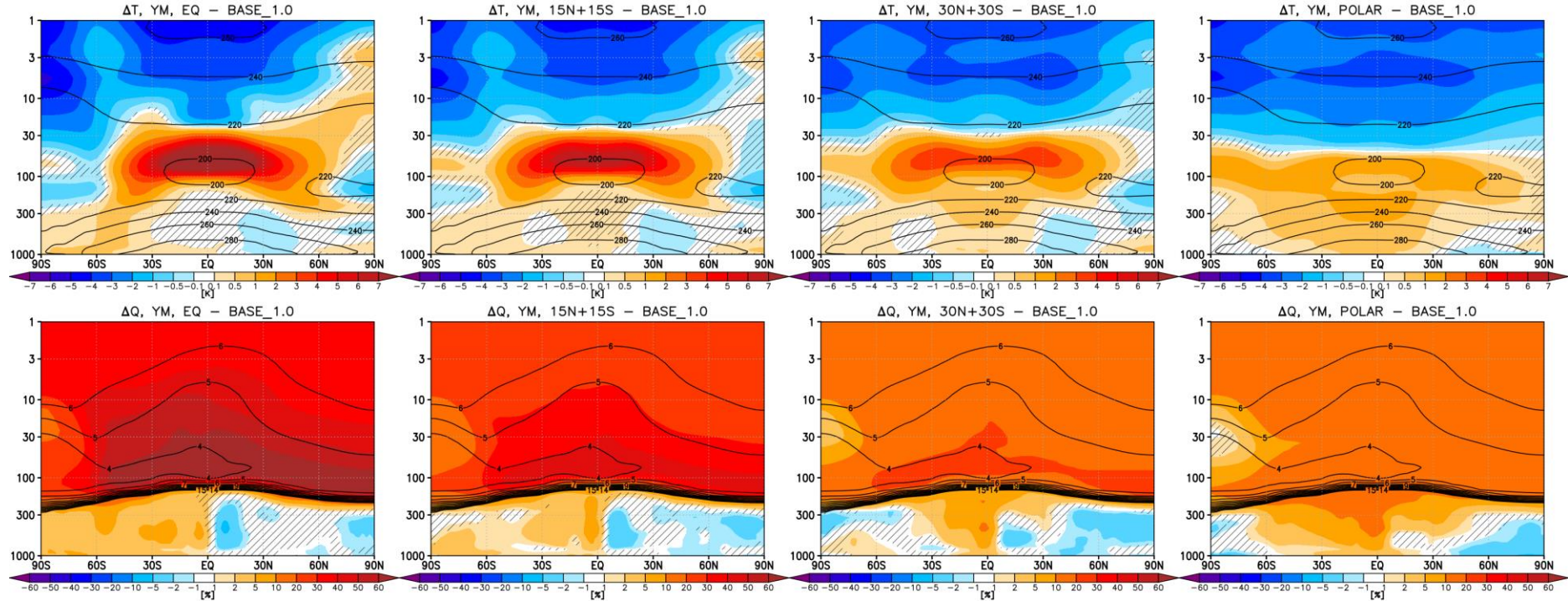


**Figure S2.** Shading: yearly mean changes in (top) temperatures and (bottom) water vapour for (left to right) EQ, 15N+15S, 30N+30S and POLAR strategy compared to the baseline period (2008-2027). Contours show the corresponding values in the baseline period for reference (in units of K and ppm for temperature and water vapour respectively). Hatching indicate regions where the response is not statistically significant, taken as smaller than  $\pm 2$  standard errors of the difference in means.



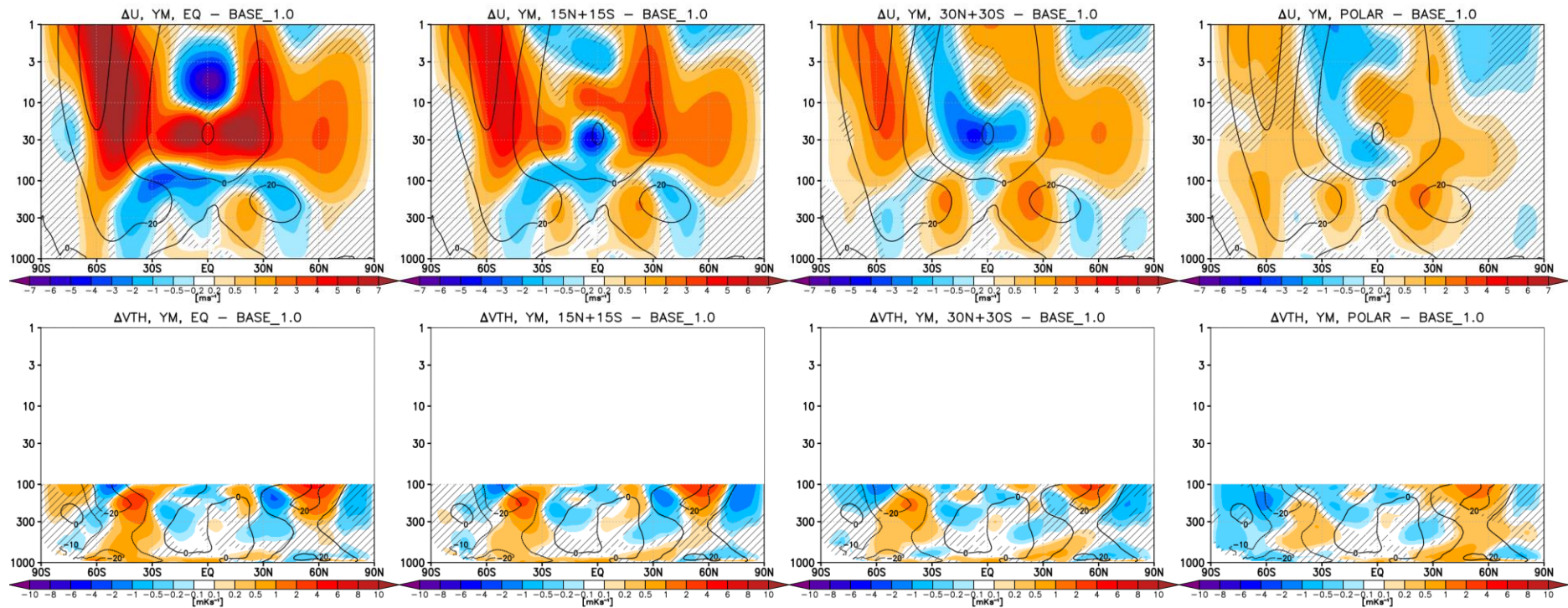


**Figure S3.** Shading: yearly mean changes in (top) zonal winds and (bottom) northward meridional eddy heat flux for (left to right) EQ, 15N+15S, 30N+30S and POLAR strategy compared to the baseline period (2008-2027). Contours show the corresponding values in the baseline period for reference. Hatching as in Fig. S2.



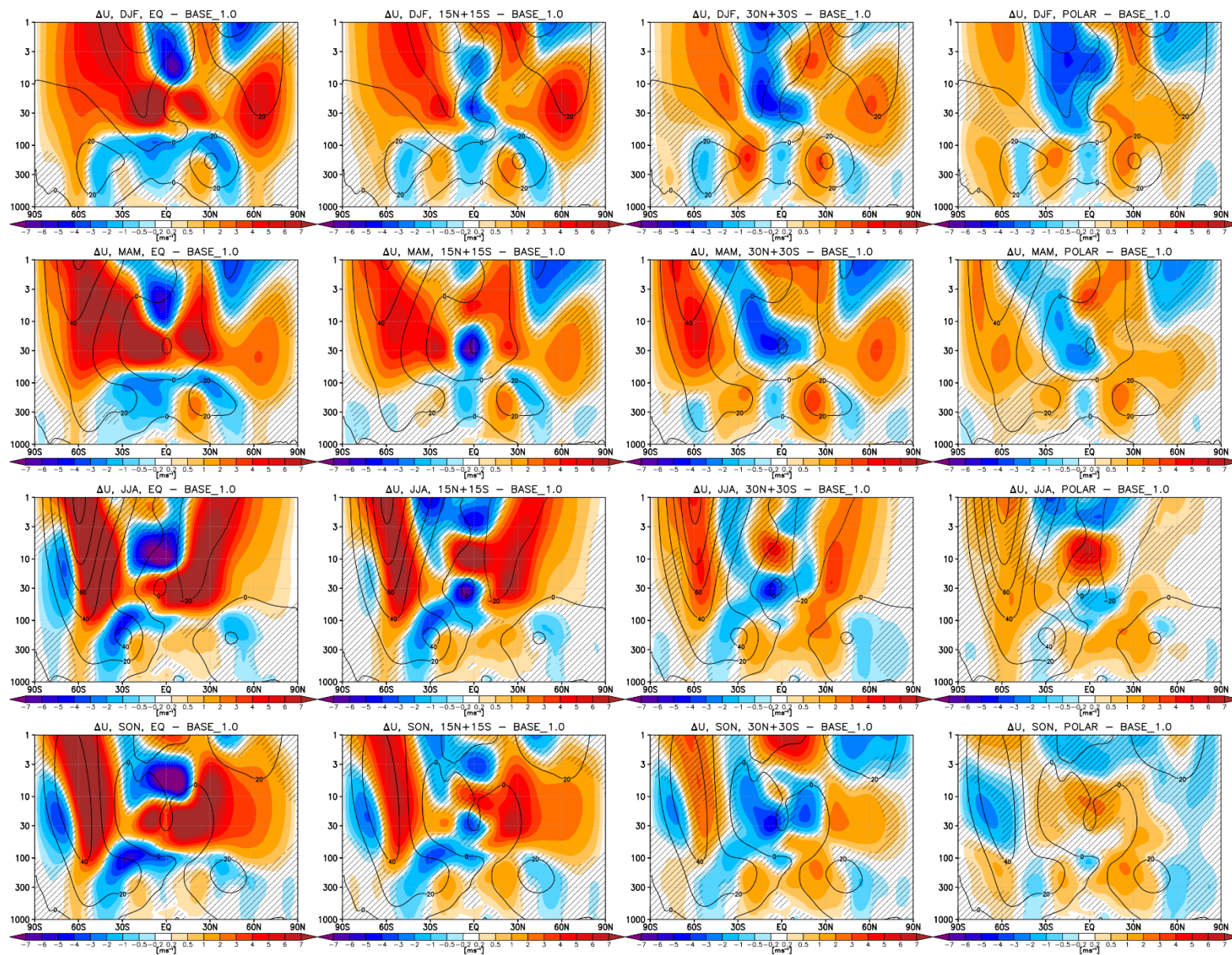


**Figure S4.** Shading: Seasonal mean (top to bottom: DJF, MAM, JJA and SON) changes in zonal winds for (left to right) EQ, 15N+15S, 30N+30S and POLAR strategy compared to the baseline period (2008-2027). Contours show the corresponding values in the baseline period for reference. Hatching as in Fig. S2.

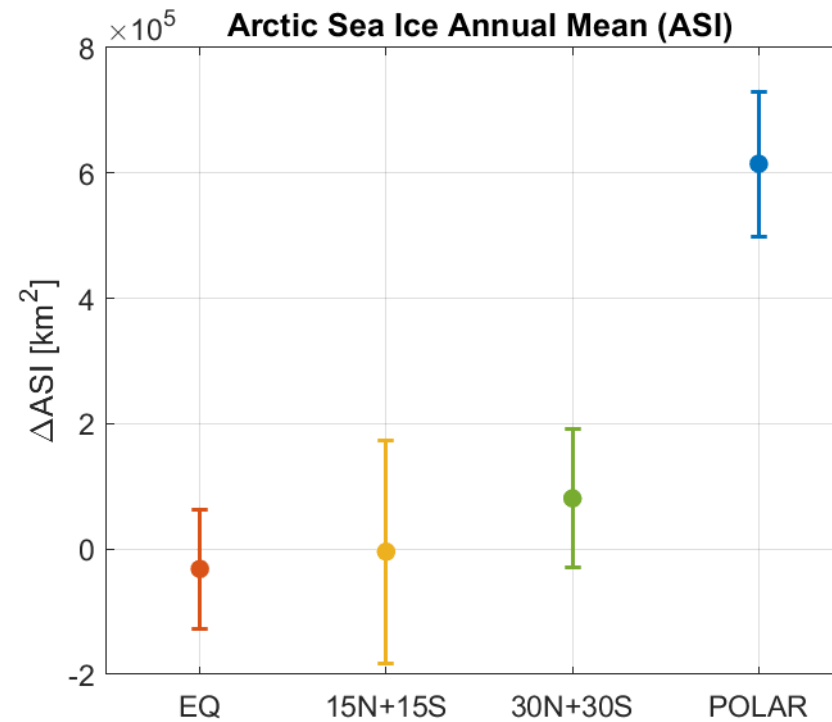


**Figure S5.** Yearly mean changes in the Arctic sea-ice extent for each of the injection strategy compared to the baseline period. The errorbars denote  $\pm 2$  standard errors of the mean of each SAI strategy.

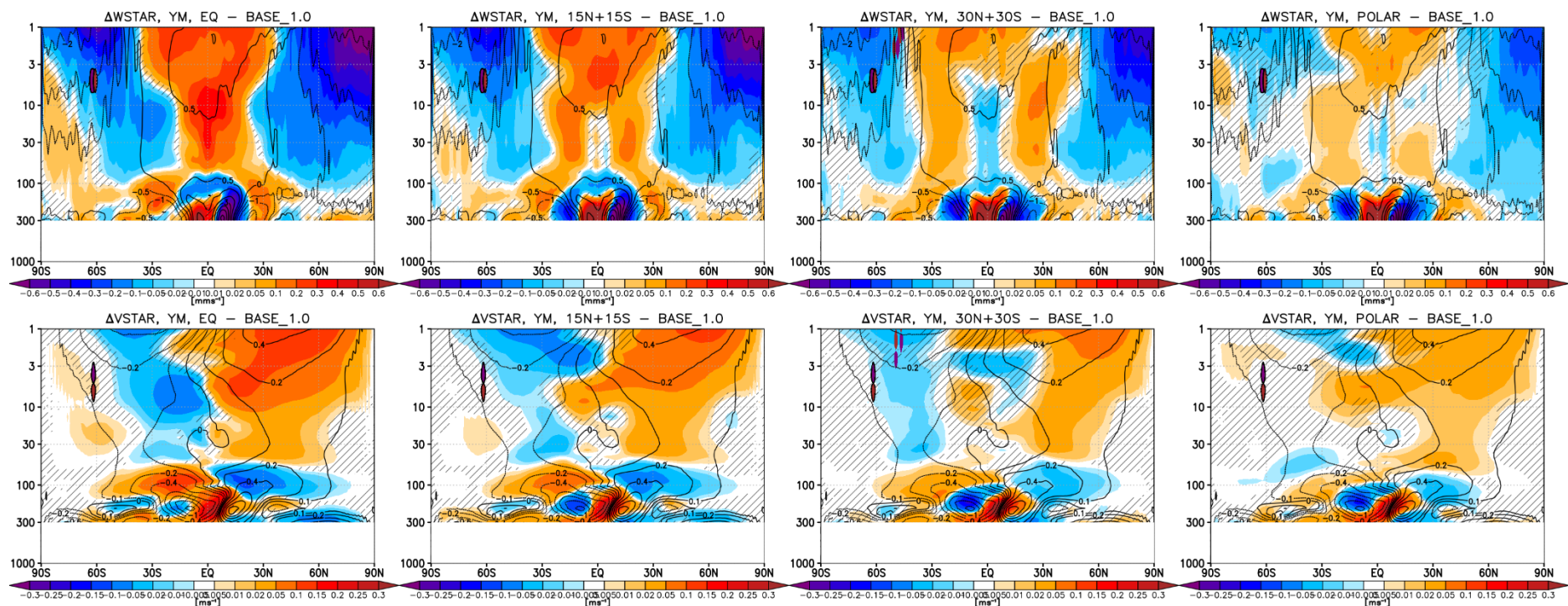


**Figure S6.** As in Fig. S2 but for the changes in TEM (top) vertical and (bottom) meridional velocities. Hatching as in Fig. S2.



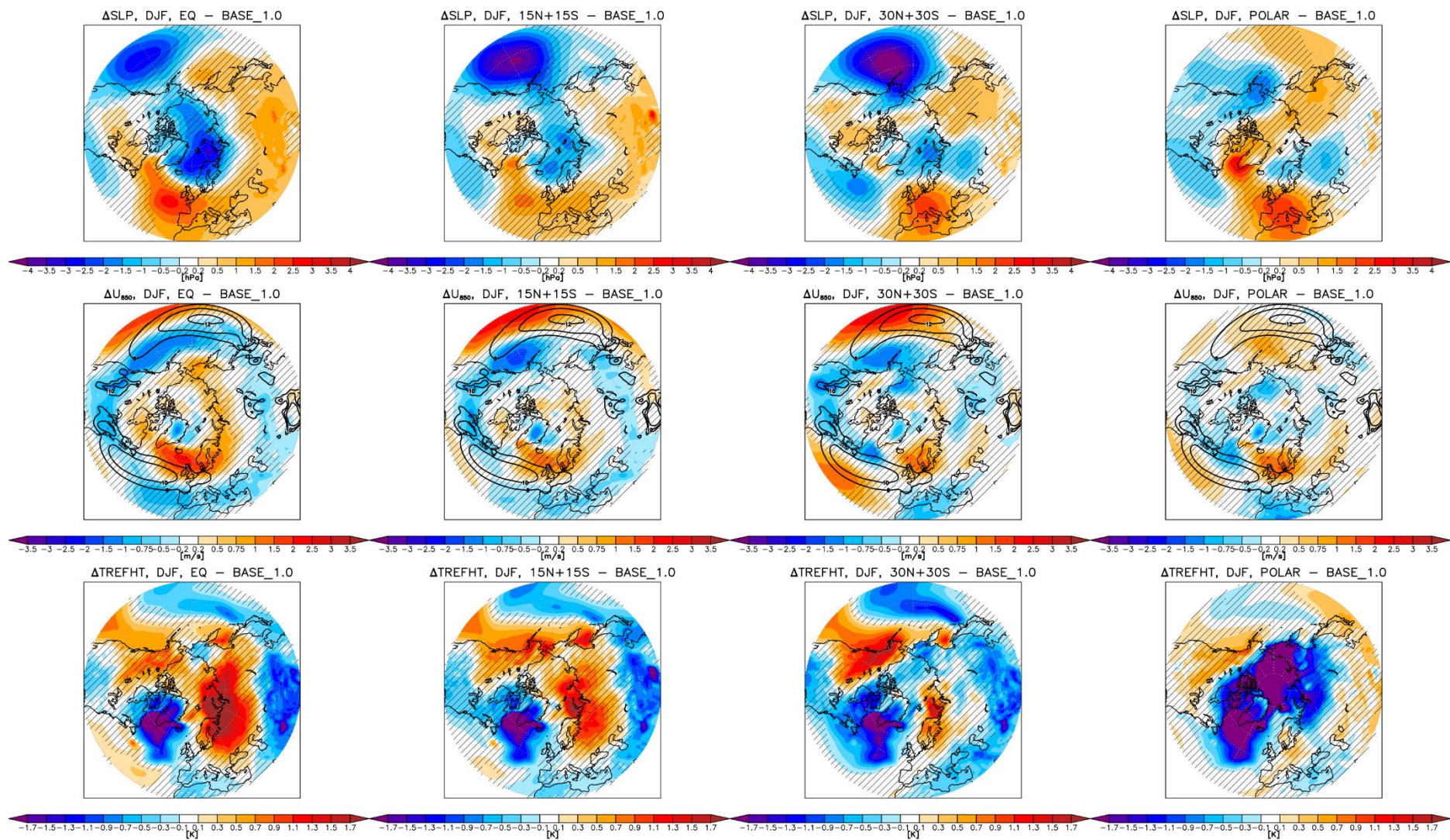


**Figure S7.** Shading: DJF mean changes in (top) sea-level pressure, (middle) zonal wind at 850 hPa and (bottom) near-surface atmospheric temperatures northward from 30°N for (left to right) EQ, 15N+15S, 30N+30S and POLAR strategy compared to the baseline period (2008 -

2027). Contours in (middle) show the corresponding values in the baseline period for reference and denote the position of the climatological jet. Hatching as in Fig. S2.

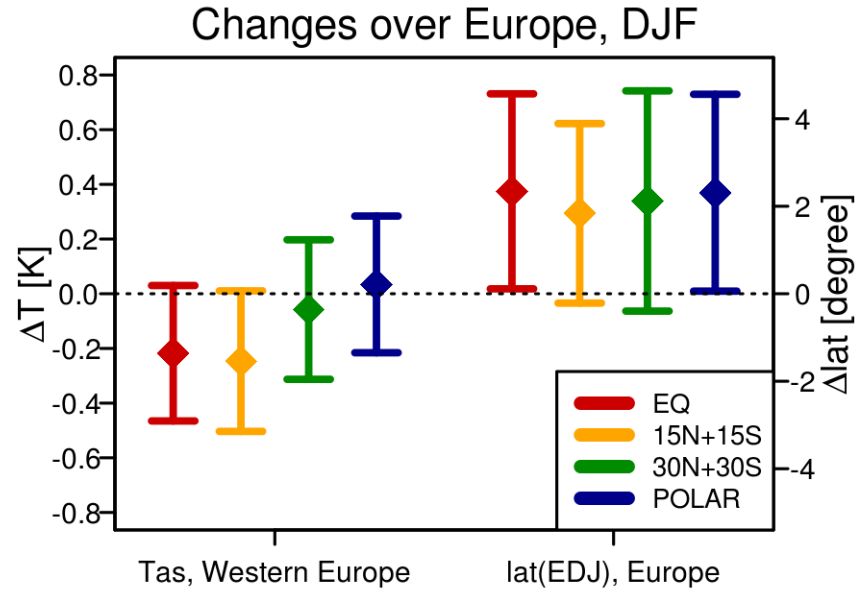


**Figure S8.** DJF mean changes in (left) near-surface atmospheric temperature over the western Europe (defined as the area spanning 10°W-10°E, 30°N-50°N) and (right) position of the NH eddy-driven jet over Europe (defined as 10°W-30°E) for each of the four strategies compared to the baseline period. The errorbars denote  $\pm 2$  standard error of the difference in means.

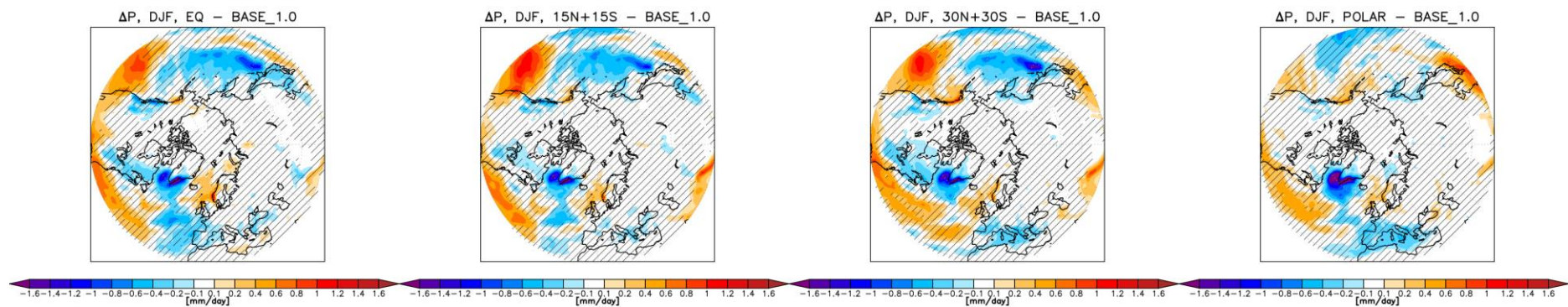


**Figure S9.** DJF mean changes in total precipitation northward from 30°N for (left to right) EQ, 15N+15S, 30N+30S and POLAR strategy compared to the baseline period (2008-2027). Hatching as in Fig. S2.



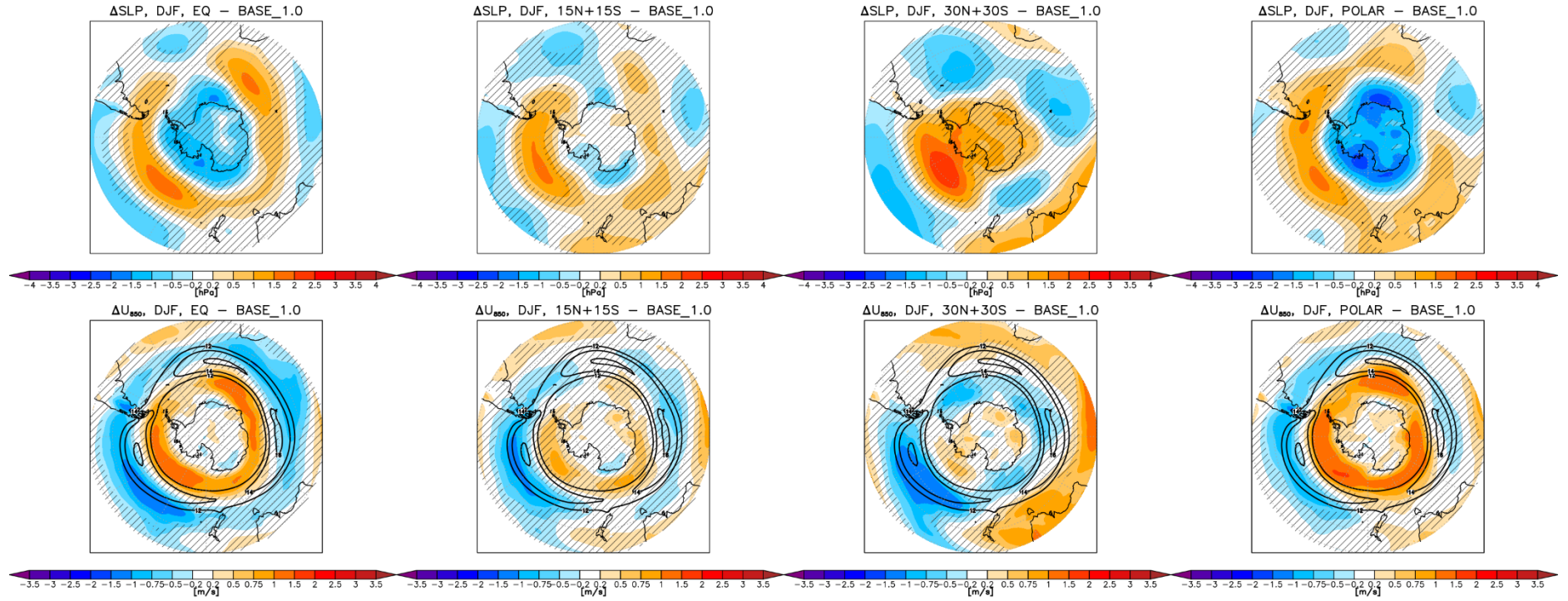


**Figure S10.** Shading: DJF mean changes in (top) sea-level pressure, and (bottom) zonal wind at 850 hPa southward from 30°S for (left to right) EQ, 15N+15S, 30N+30S and POLAR strategy compared to the baseline period (2008-2027). Contours in (bottom) show the corresponding values in the baseline period for reference and denote the position of the climatological jet. Hatching as in Fig. S2.



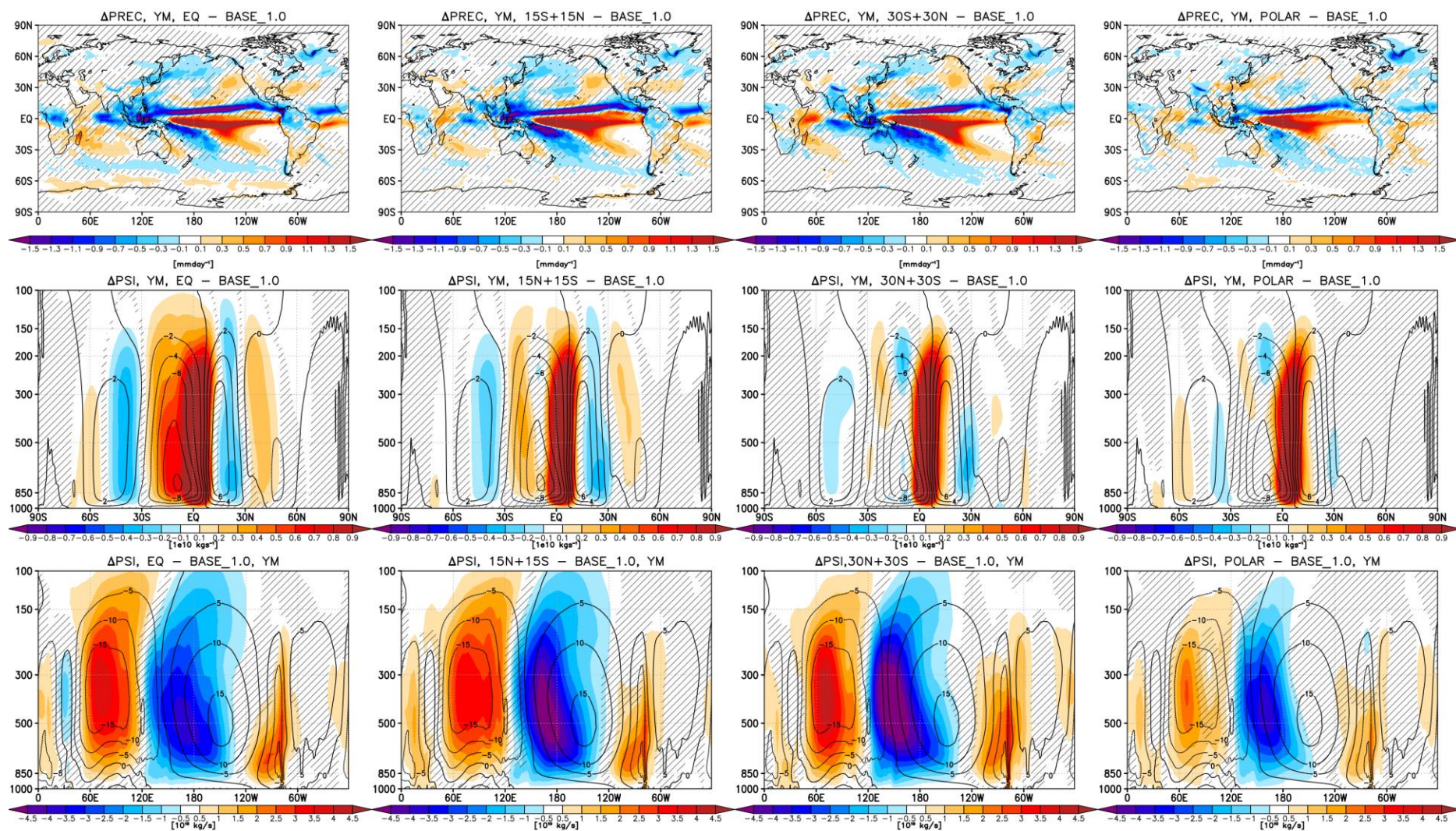


**Figure S11.** Shading: Yearly mean changes in (top) precipitation, (middle) meridional mass stream function, and (bottom) zonal mass stream function for (left to right) EQ, 15N+15S, 30N+30S and POLAR strategy compared to the baseline period (2008-2027). Contours show the corresponding values in the baseline period for reference. Hatching as in Fig. S2.

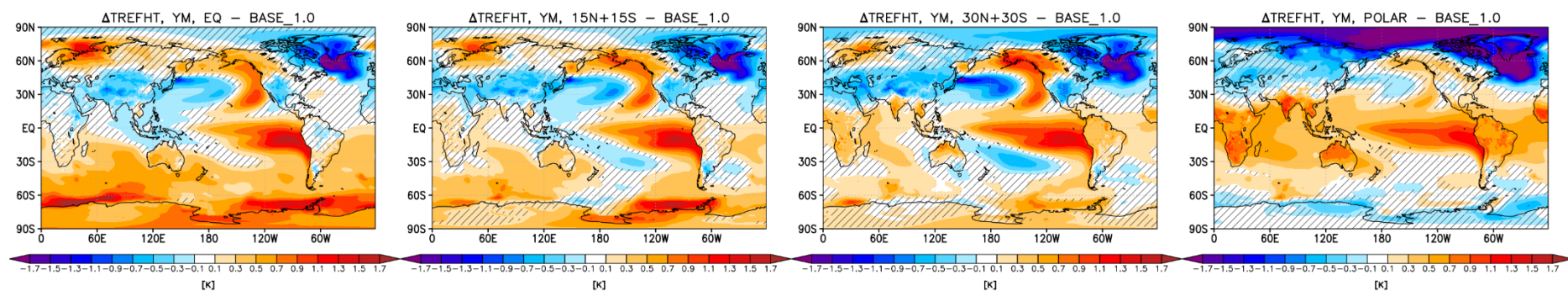


**Figure S12.** Yearly mean changes in near-surface air temperatures for (left to right) EQ, 15N+15S, 30N+30S and POLAR strategy compared to the baseline period. Hatching as in Fig. S2.



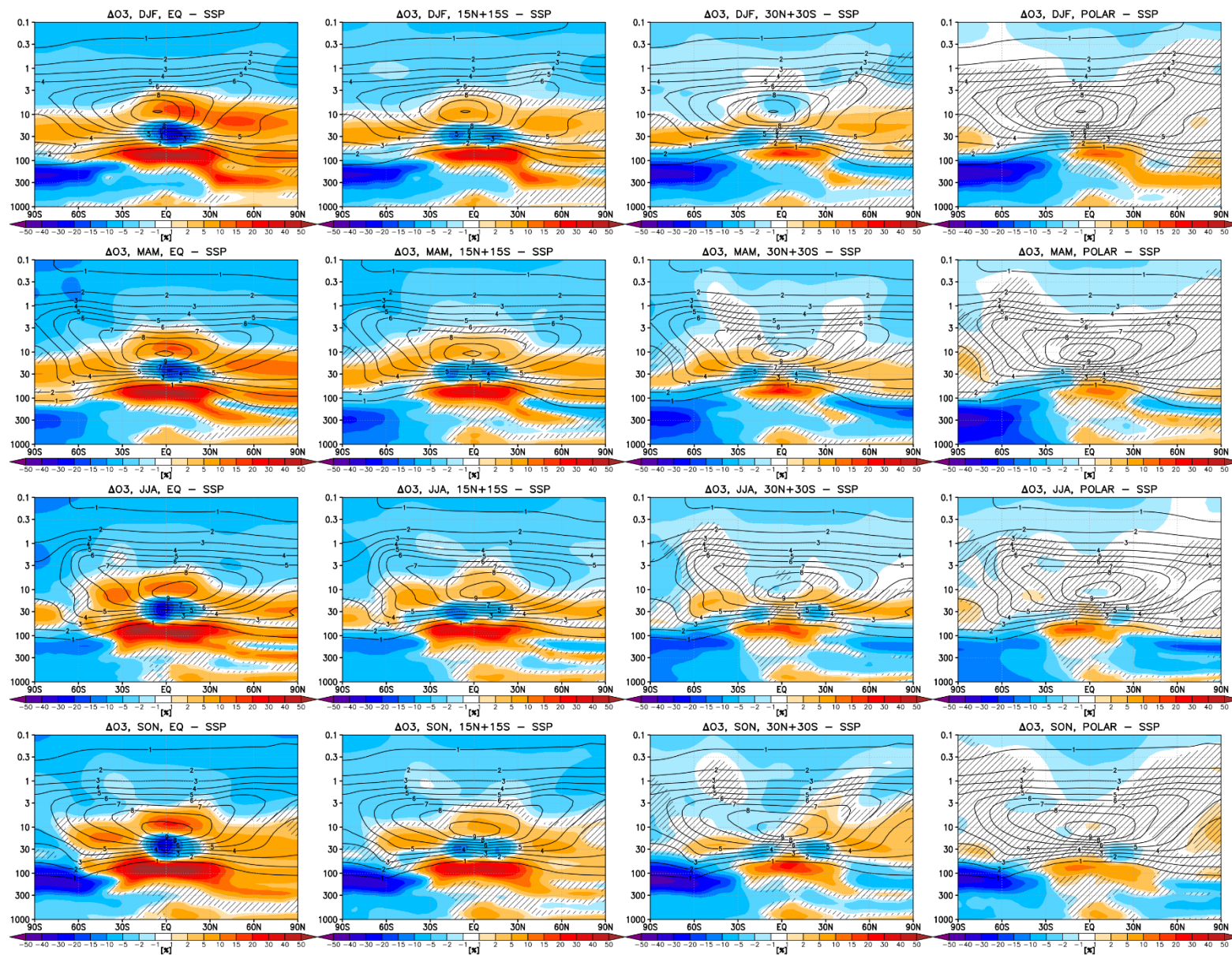


**Figure S13.** Shading: Seasonal mean (top to bottom: DJF, MAM, JJA and SON) changes in ozone mixing ratios (left to right) EQ, 15N+15S, 30N+30S and POLAR strategy compared to the same period (i.e. 2050-2069) of the control SSP2-4.5 simulation. Contours show the corresponding values in SSP2-4.5 for reference (in the units of ppm). Hatching as in Fig. S2.